

Diffraction of X-ray free-electron laser femtosecond pulses on single crystals in the Bragg and Laue geometry

V. A. Bushuev

M. V. Lomonosov Moscow State University, 119992 GSP-2 Moscow, Russia.

E-mail: vabushuev@yandex.ru

A solution of the problem of dynamical diffraction for X-ray pulses with arbitrary dimensions in the Bragg and Laue cases in a crystal of any thickness and asymmetry coefficient of reflection is presented. Analysis of pulse form and duration transformation in the process of diffraction and propagation in a vacuum is conducted. It is shown that only the symmetrical Bragg case can be used to avoid smearing of reflected pulses.

© 2008 International Union of Crystallography
Printed in Singapore – all rights reserved

Keywords: free-electron lasers; ultrashort X-ray pulses; X-ray optics; dynamical diffraction.

1. Introduction

In the near future, X-ray free-electron lasers (XFELs) with wavelength $\lambda \simeq 0.1$ nm will become available for a wide community of users. Therefore it is of interest to consider dynamical diffraction as a tool for controlling and tailoring parameters of femtosecond pulses and for developing methods of X-ray laser pulse diagnostics. Three XFEL projects are now actively developed: the European XFEL Facility in Germany (Altarelli *et al.*, 2006), the LCLS (Linac Coherent Light Source) in the USA (Arthur *et al.*, 2002) and the SCSS (SPring-8 Compact SASE Source) in Japan (Tanaka & Shintake, 2005). In these machines, X-ray bunches of duration ~ 100 – 200 fs leave an undulator as a result of self-amplification of spontaneous radiation of 15 GeV electrons. Theoretical calculations show that these pulses will have an irregular multiple-peak internal structure and consist of several hundreds of supershort independent sub-pulses of duration $\tau_0 \simeq 0.1$ fs, separated by time intervals $\Delta t \simeq 0.3$ – 0.5 fs. A typical pulse has a transversal size $r_0 \simeq 50$ μm at the undulator exit, angular divergence $\simeq 1$ μrad , peak power $\simeq 10$ GW and average power $\simeq 40$ W (Saldin *et al.*, 2004).

The analysis of diffraction of XFEL radiation has been restricted so far to the approximation of a plane (unlimited) wavefront for the Bragg case (Chukhovskii & Förster, 1995; Shastri *et al.*, 2001*a,b*; Graeff, 2004) and for the Laue case (Shastri *et al.*, 2001*b*; Graeff, 2002; Malgrange & Graeff, 2003). The time structure of the incident pulse has been approximated either by a δ function (Chukhovskii & Förster, 1995; Shastri *et al.*, 2001*a,b*; Graeff, 2002; Malgrange & Graeff, 2003) or by a Gaussian (Shastri *et al.*, 2001*a*; Graeff, 2004). Although giving some insight into the physics of short-pulse diffraction, such an approach cannot in principle take into account the presence of transverse mode structure and, even more essential, a non-uniform distribution of the field phase inside a

pulse. However, such a phase distribution will inevitably arise at large, of the order of 100 m (Saldin *et al.*, 2004), distances from the undulator to the sample or monochromator crystal. Besides, all analysis so far has been limited to the reflected pulse field on the exit surface of a crystal, whereas significant practical interest is for spatial (transversal) and temporal (longitudinal) smearing of pulses during their further propagation in vacuum.

In the present article a general theory of dynamical diffraction of X-ray pulses with an arbitrary spatial and temporal structure, described by a field $\mathbf{E}_{\text{in}}(\mathbf{r}, t)$, on crystals with arbitrary thickness and asymmetry coefficient in the Bragg and in the Laue cases is developed. Such an approach allows us to analyse the structure of fields $\mathbf{E}_g(\mathbf{r}, t)$ of forward-diffracted (transmitted, $g = 0$) and diffracted (reflected, $g = h$) pulses at any distance from the crystal, and also the degree of space and time coherence of these pulses and their relation with the statistical properties of the XFEL radiation field.

2. Theory

We shall consider diffraction reflection and transmission of a pulse of X-ray radiation $E_{\text{in}}(\mathbf{r}, t) = A_{\text{in}}(\mathbf{r}, t) \exp(i\mathbf{K}_0\mathbf{r} - i\omega_0 t)$, which is incident on a single-crystal plate of thickness d . The field on the entrance crystal surface $z = 0$ can be written as

$$E_{\text{in}}(x, t) = A_{\text{in}}(x, t) \exp(iK_{0x}x - i\omega_0 t), \quad (1)$$

where $A_{\text{in}}(x, t)$ is a slowly varying complex amplitude (the envelope of a wave packet), $K_{0x} = K_0 \sin \theta_0$, $K_0 = \omega_0/c = 2\pi/\lambda$ and c is the light speed in a vacuum; the axis x is directed along the crystal surface and the axis z is directed inside the crystal along the normal \mathbf{n} to the surface (Fig. 1). The projection of the incident wavevector on the axis z is $K_{0z} = K_0 \gamma_0$, where $\gamma_0 = \cos(\mathbf{K}_0 \cdot \mathbf{n}) = \cos \theta_0$. The angle of incidence of the radiation to

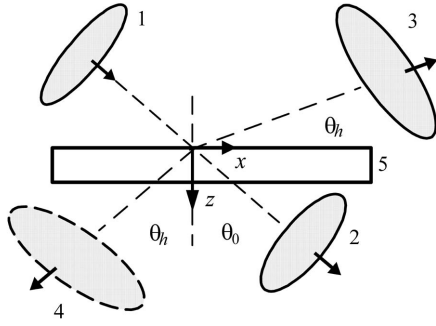


Figure 1
Geometry in real space of X-ray pulse diffraction in the Bragg and Laue cases. 1, incident pulse $E_{in}(\mathbf{r}, t)$; 2, transmitted pulse $E_0(\mathbf{r}, t)$; 3, reflected pulse $E_h(\mathbf{r}, t)$ in the Bragg case; 4, reflected pulse in the Laue case; 5, crystal; θ_0 and θ_h are the angle of incidence of the initial pulse and the angle of reflection of the diffracted pulse, respectively, relative to the axis z .

the normal \mathbf{n} is $\theta_0 = \psi - \theta_B - \Delta\theta$, where θ_B is the Bragg angle for the central (average) frequency ω_0 , which is determined by the expression $2K_0 \sin \theta_B = h$, where h is the modulus of the reciprocal lattice vector $\mathbf{h} = (h \cos \psi, -h \sin \psi)$, $\Delta\theta$ is the angular deviation from the exact Bragg angle, which is determined by the expression $\mathbf{K}_0 \mathbf{h} = -K_0 h \sin(\theta_B + \Delta\theta)$, and ψ is the inclination angle of reflecting crystal planes to the normal \mathbf{n} . The restriction $|\psi - \theta_B| < \pi/2$ on angle ψ follows from the condition $\gamma_0 > 0$. Representation of a pulse by the form (1) is correct as long as the characteristic cross-section size of a pulse $r_0 \gg \lambda$, and its duration $\tau_0 \gg \lambda/c$.

Let us now write the field $E_{in}(x, t)$ (1) in the form of a two-dimensional Fourier integral,

$$E_{in}(x, t) = \iint E_{in}(k_{0x}, \omega) \exp(ik_{0x}x - i\omega t) dk_{0x} d\omega, \quad (2)$$

where

$$E_{in}(k_{0x}, \omega) = (2\pi)^{-2} \iint E_{in}(x, t) \exp(-ik_{0x}x + i\omega t) dx dt. \quad (3)$$

Here and further on, all integrations are carried out over the infinite limits from $-\infty$ to $+\infty$. Substituting the field $E_{in}(x, t)$ (1) into (3) and introducing new variables

$$q = k_{0x} - K_{0x}, \quad \Omega = \omega - \omega_0, \quad (4)$$

one obtains a set of Fourier amplitudes of the field, $E_{in}(k_{0x}, \omega) = A_{in}(q, \Omega)$, with

$$A_{in}(q, \Omega) = (2\pi)^{-2} \iint A_{in}(x, t) \exp(-iqx + i\Omega t) dx dt. \quad (5)$$

Expression (2) describes a set of plain monochromatic waves with amplitudes $A_{in}(q, \Omega)$, wavevectors $\mathbf{k}_0 = (k_{0x}, k_{0z})$ and frequencies ω , where $k_{0x} = K_{0x} + q$, $k_{0z} = (k_0^2 - k_{0x}^2)^{1/2}$ and $k_0 = (\omega_0 + \Omega)/c$, which are incident on a crystal surface. In accordance with the known results of the plane-wave dynamical theory of X-ray diffraction, each single component wave in (2) is transmitted and reflected with the amplitude coefficients of transmission $T(q, \Omega)$ and reflection $R(q, \Omega)$. As a result we shall obtain the distribution of fields $E_g(x, z, t)$ for transmitted ($g = 0$) and reflected ($g = h$) pulses at any point of space (x, z) outside the crystal and at any moment of time t ,

$$E_g(\mathbf{r}, t) = \iint B_g(q, \Omega) A_{in}(q, \Omega) \exp(i\mathbf{k}_g \mathbf{r} - i\omega t) dq d\Omega, \quad (6)$$

where $B_0 = T$, $B_h = R$.

Here it is taken into account that owing to a condition of continuity of the tangential components of the wavevectors at the entrance and exit crystal surfaces, the values of projections of wavevectors \mathbf{k}_g in a vacuum will take the following form,

$$k_{gx} = K_{gx} + q, \quad k_{gz} = \sigma_g (k_0^2 - k_{gx}^2)^{1/2}, \quad (7)$$

where $K_{gx} = K_{0x} + g_x$, $g = 0, h$; $\sigma_{0,h} = 1$ in the Laue case; $\sigma_0 = 1$ and $\sigma_h = -1$ in the Bragg case; $z \leq 0$ for a reflected pulse in the Bragg case and $z \geq d$ in the Laue case and for a transmitted pulse in the Bragg case. Contrary to the usual notation of wavevectors, namely denoting wavevectors in a vacuum by \mathbf{K}_g and in the crystal by \mathbf{k}_g , \mathbf{K}_g denotes the average wavevectors of the pulses and \mathbf{k}_g takes into account the q - and ω -spectra of the incident, reflected and transmitted pulses. Throughout this paper all wavevectors are restricted to a vacuum.

Note that the Fourier-transform-based approach, used here, is more simple and productive in comparison with the time-dependent Takagi-Taupin differential equations used by Chukhovskii & Förster (1995), Wark & He (1994) and Wark & Lee (1999).

Representing the square root (7) in the form of a series over small parameters q/K_0 and Ω/ω_0 , which is truncated discarding terms of the third order and higher, and substituting this result into the two-dimensional integral (6), we obtain a general expression for the electric fields of X-ray pulses [see Appendix A, equations (30) and (31)],

$$E_g(\mathbf{r}, t) = A_g(\mathbf{r}, t) \exp(i\mathbf{K}_g \mathbf{r} - i\omega_0 t), \quad (8)$$

where $K_{gx} = K_{0x} + g_x = K_0 \sin \theta_g$, $K_{gz} = \sigma_g (K_0^2 - K_{gx}^2)^{1/2} = K_0 \gamma_g$, $\gamma_g = \cos \theta_g$. The angle of diffraction reflection with respect to the crystal normal is $\theta_h = \psi + \theta_B - b \Delta\theta$, where $b = \gamma_0/\gamma_h$ is the asymmetry coefficient of the reflection. In the Bragg case, $\gamma_h < 0$, $b < 0$, and angle ψ must satisfy the condition $|\psi - \pi/2| < \theta_B$. The slow-varying amplitudes are

$$A_g(x, z, t) = \iint B_g(q, \Omega) A_{in}(q, \Omega) \exp(iS_g + iD_g) dq d\Omega, \quad (9)$$

where

$$S_g(q, \Omega) = q(x - \tan \theta_g z) - \Omega(t - z/c\gamma_g), \quad (10)$$

$$D_g(q, \Omega) = -[q - (\Omega/c) \sin \theta_g]^2 z / (2K_0 \gamma_g^3). \quad (11)$$

The phase S_g (10) determines the displacement of pulse centres in x and t with distance z from the crystal. The phase D_g (11), which is quadratic in $[q - (\Omega/c) \sin \theta_g]$ and proportional to z , describes the curvature of the wavefront and the diffraction smearing of pulses during their propagation in a vacuum. It is necessary to take into account the terms of the order of $\sim q^2$, Ω^2 and $q\Omega$ to obtain a correct solution of expression (7) and to analyse diffraction broadening of pulses in space and in time. In all previous articles this extremely important aspect was not taken into account. Expression (11) describes the effect of the curvature of the asymptotes of the dispersion surface far away from the reflecting crystal for pulses limited in time and in space. The influence of curved

asymptotes has been considered theoretically earlier, for example, by Bauspiess *et al.* (1976) in the case of the incident spherical X-ray or neutron waves on the interferometer. Integral (9) is equivalent to the integral formula of Kirchhoff–Helmholtz, generalizing the Huygens–Fresnel principle, since in the quasi-optical approximation the spherical wavefront of point sources can be replaced by a parabolic wavefront, which is justified in the paraxial region.

Let us write the reflection coefficient $R(q, \Omega)$ and transmission coefficient $T(q, \Omega)$ in (6) and in (9) for a crystal with any thickness d in the general form. In the Bragg case,

$$\begin{aligned} R &= (R_1 - pR_2)/(1 - p), \\ T &= [\exp(i\varphi_1) - p \exp(i\varphi_2)]/(1 - p), \end{aligned} \quad (12)$$

where

$$\begin{aligned} R_{1,2} &= (\alpha_1 \pm Q)/2C\chi_{\bar{h}}, & p &= (R_1/R_2) \exp[i(\varphi_1 - \varphi_2)], \\ \varphi_{1,2} &= k_0 \varepsilon_{1,2} d, & \varepsilon_{1,2} &= (2\chi_0 + \alpha_1 \pm Q)/4\gamma_0, \\ \alpha_1 &= \alpha b - \chi_0(1 - b), & Q &= (\alpha_1^2 + 4bC^2\chi_h\chi_{\bar{h}})^{1/2}. \end{aligned}$$

Here χ_g are the Fourier components of the dielectric susceptibility of the crystal; $C = 1$ and $C = \cos 2\theta_B$ for σ - and π -polarized radiation, respectively. Parameter $\alpha = [k_0^2 - (\mathbf{k}_0 + \mathbf{h})^2]/k_0^2$, determining the deviation from the exact Bragg condition, has the form

$$\begin{aligned} \alpha(q, \Omega) &= 2 \sin 2\theta_B [\Delta\theta - q/K_0\gamma_0 \\ &\quad + (\Omega/\omega_0) \sin \psi/\gamma_0 \cos \theta_B], \end{aligned} \quad (13)$$

where $\Delta\theta$ is the departure of the incident pulse from the Bragg angle.

In the Laue case,

$$B_g = A_g^{(1)} \exp(i\varphi_1) + A_g^{(2)} \exp(i\varphi_2), \quad (14)$$

where

$$A_0^{(1,2)} = (Q \mp \alpha_1)/2Q, \quad A_h^{(1,2)} = \pm Cb\chi_h/Q.$$

The characteristic angular width $\Delta\theta_B$ of the diffraction reflection coefficients R (12) and $R = B_h$ (14) depends on the ratio between the thickness of the crystal d and the extinction length $\Lambda = \lambda(\gamma_0|\gamma_h|)^{1/2}/\pi C|\chi_h|$. In the case of a thick crystal ($d \gg \Lambda$) this width is equal to $\Delta\theta_B = C|\chi_h|/|b|^{1/2} \sin 2\theta_B$, or, in the other designations, $\Delta\theta_B = \lambda|\gamma_h|/\pi\Lambda \sin 2\theta_B$. In the case of a thin crystal, when $d \leq \Lambda$, the angular width of the reflection is $\Delta\theta_B \simeq \lambda|\gamma_h|/\pi d \sin 2\theta_B$. The reflection coefficient in the Laue case is maximal if the crystal thickness satisfies the condition $d = (\pi/2)\Lambda(1 + 2n)$, where $n = 0, 1, 2, \dots$

The intensities of the transmitted and reflected pulses are determined by the expression $I_g(x, z, t) = |A_g|^2$. It is easy to show that the total energy of a pulse, $W_g = \iint I_g dx dt$, does not depend on the distance z and the time t , which means conservation of energy during the pulse propagation in a vacuum,

$$W_g = (2\pi)^2 \iint |B_g(q, \Omega)|^2 |A_{in}(q, \Omega)|^2 dq d\Omega.$$

As an example, we shall further consider everywhere a Gaussian incident pulse,

$$\begin{aligned} A_{in}(x, t) &= \exp[-(x\gamma_0/r_0)^2 + i\varphi_0(x) \\ &\quad - (t - x \sin \theta_0/c)^2/\tau_0^2], \end{aligned} \quad (15)$$

where r_0 and τ_0 are the transverse size and the pulse duration of the incident pulse, respectively, $\varphi_0(x) = \alpha_0(x\gamma_0/r_0)^2$ is the phase, and the parameter α_0 is equal to the phase at $|x| = r_0/\gamma_0$ [see Appendix B, expression (45)].

Depending on the ratio between r_0 and τ_0 it is possible to introduce the concept of a long pulse, for which pulse duration $\tau_0 \gg (r_0/c) \tan \theta_0$, and a short pulse with wide front with $r_0 \gg c\tau_0 \cotan \theta_0$. In the first case, only a limited area of the crystal surface with $|x| \leq x_0 = r_0/\gamma_0$ is involved in the scattering, whereas in the second case the incident pulse with size $\Delta x \simeq c\tau_0/\sin \theta_0 \ll x_0$ propagates along the crystal surface with speed $c/\sin \theta_0$, higher than the speed of light in a vacuum. It is the latter situation that will be realised for femtosecond pulses.

For narrow and short pulses the angular divergence $\Delta\theta_0 \simeq \lambda/\pi r_0$ and spectral width $\Delta\Omega_0 \simeq 2/\tau_0$ are comparable or even exceed the angular width $\Delta\theta_B$ and spectral width $\Delta\Omega_B = \Delta\theta_B \omega_0 \cotan \theta_B$ of a Bragg reflection. This leads to a sharp change in the form and to reduction of intensity of a reflected pulse, but also to its smearing in time as well as in space. The degree of smearing in the general case increases with the distance z (see §3).

3. Results and discussion

Let us explore some examples of typical pulse parameters. We shall always consider the 220 reflection of σ -polarized radiation with $\lambda = 0.154$ nm from a silicon single crystal at a departure angle $\Delta\theta = (1 - b) \text{Re}(\chi_0)/2 \sin 2\theta_B$, which corresponds to the maximal reflected intensity, where $\theta_B = 23.65^\circ$. In the symmetric Bragg case ($b = -1$), the Bragg width for a thick crystal $\Delta\theta_B = 12.4 \mu\text{rad}$, and the extinction length $\Lambda = 2.16 \mu\text{m}$. In the symmetric Laue case ($b = 1$), $\Lambda = 4.92 \mu\text{m}$. From a general point of view it is clear that for the reduction of heat absorption the thickness of a crystal should best be chosen small ($d \leq 1-3\Lambda$), but at the same time large enough to provide sufficiently high X-ray reflection coefficient values.

The expressions (8)–(14) give a general solution of the problem of transmission and reflection of X-ray pulses in the Bragg and Laue cases. Let us discuss some special cases. If the field amplitude A_{in} does not depend on x and t , then, in agreement with expressions (5) and (13), $A_{in}(q, \Omega) = \delta(q)\delta(\Omega)$, $\alpha = 2\Delta\theta \sin 2\theta_B$, and we find the well known result for a plane monochromatic wave: $A_g = B_g(\Delta\theta)$. Formally this means that in (15) one should assume $r_0 \rightarrow \infty$ and $\tau_0 \rightarrow \infty$. In a real situation the approximation of a plane monochromatic wave will be realised at $\Delta\theta_0 \ll \Delta\theta_B$ and $\Delta\Omega_0 \ll \Delta\Omega_B$, *i.e.* in the case of a source of size $r_s \gg \lambda/(\pi\Delta\theta_B)$ [see expression (44) at $\alpha_s = 0$] and of pulse duration $\tau_0 \gg 2/\Delta\Omega_B$. For example, for $\lambda = 0.154$ nm in the case of symmetric Bragg reflection Si(220) this leads to the following requirements: $r_0 \gg 4 \mu\text{m}$, $\tau_0 \gg 6$ fs.

For a less restrictive approximation of a monochromatic X-ray beam, the amplitude $A_{in}(x)$ depends only on one coordinate, *i.e.* $\tau_0 \rightarrow \infty$ in equation (15). In this case, $A_{in}(q, \Omega) = A_{in}(q)\delta(\Omega)$, $\alpha = 2 \sin 2\theta_B(\Delta\theta - q/K_0\gamma_0)$ and

$$A_g(x, z) = \int B_g(q)A_{\text{in}}(q) \exp(iS_g + iD_g) dq, \quad (16)$$

where

$$S_g = q(x - \tan \theta_g z), \quad D_g = -q^2 z / (2K_0 \gamma_g^3).$$

Expression (16), which is valid at any z and d , is more general in comparison with that obtained earlier using the Green function method for diffraction reflection of a limited X-ray beam from a semi-infinite crystal at $z = 0$ in the Bragg case (Afanas'ev & Kohn, 1971) and at $z = d$ in the Laue case (Slobodetzki & Chukhovskii, 1970).

It is of further interest to analyse diffraction of a short pulse with a wide wavefront when the longitudinal size of the incident pulse $l_0 = c\tau_0 \ll r_0$. In this case it is possible to neglect boundary effects, *i.e.* to exclude the field dependence on the incident pulse transverse coordinate. Then $A_{\text{in}}(x, t) = A_{\text{in}}(t - x \sin \theta_0 / c)$ and, in agreement with (5), $A_{\text{in}}(q, \Omega) = A_{\text{in}}(\Omega) \delta(q - \Omega \sin \theta_0 / c)$. As a result, from (9) it is easy to show that

$$A_g(x, z, t) = \int B_g(\Omega)A_{\text{in}}(\Omega) \exp(iS_g + iD_g) d\Omega, \quad (17)$$

where

$$S_g = (\Omega/c) [\sin \theta_0 x + (1 - \sin \theta_0 \sin \theta_g) z / \gamma_g] - \Omega t, \quad (18)$$

$$D_g = -\Omega^2 F_g z, \quad F_g = (\sin \theta_0 - \sin \theta_g)^2 / (2K_0 c^2 \gamma_g^3). \quad (19)$$

The substitution of expression $q = \Omega \sin \theta_0 / c$ into (13) results in a known expression for the value of α in the case of an incident non-monochromatic plane wave,

$$\alpha(\Omega) = 2 \sin 2\theta_B [\Delta\theta + (\Omega/\omega_0) \tan \theta_B]. \quad (20)$$

For convenience, the analysis of the space and time structure of amplitudes $A_g(x, z, t)$ (17) can be carried out in a new Cartesian system of coordinates (x'_g, z'_g) with transition rules $x = x'_g \cos \varphi'_g + z'_g \sin \varphi'_g$, $z = z'_g \cos \varphi'_g - x'_g \sin \varphi'_g$, in which the axis z'_g makes an angle φ'_g with the crystal normal \mathbf{n} . This angle φ'_g is selected in such a way that the phase S_g (18) becomes independent of the transversal coordinate x'_g . From (18) it is easy to obtain

$$\tan \varphi'_g = \gamma_g \sin \theta_0 / (1 - \sin \theta_0 \sin \theta_g). \quad (21)$$

Note that the axes of coordinates (x'_h, z'_h) and (x_p, z_p) in Appendix C are parallel to each other; however, the system (x_p, z_p) moves with the speed of light in a vacuum along the direction of the wavevector \mathbf{K}_h [see Fig. 8 and the formulae (53), (55)]. It is easy to be convinced that the angle $\varphi'_h = \theta_h + \varphi_h$, where the angle φ_h is defined from equation (56).

In the new coordinate system the phase $S_g = -\Omega(t - z'_g/V_g)$, where V_g is the speed of the pulse along the longitudinal axis z'_g ,

$$V_g = c|\gamma_g| / (1 - 2 \sin \theta_0 \sin \theta_g + \sin^2 \theta_0)^{1/2}. \quad (22)$$

From expressions (19), (21) and (22) it follows that, for transmitted pulses ($g = 0$) both in the Bragg case and in the Laue case, $\varphi'_0 = \theta_0$, $V_0 = c$ and $D_0 = 0$. In other words the incident pulse with a wide front is transmitted along its initial direction \mathbf{K}_0 with the speed of light and is not deformed during the pulse transmission in a vacuum, *i.e.* remains a plane non-

monochromatic wave with time dependence $A_0(t - z_0'/c)$, which differs in the general case from $A_{\text{in}}(t - z_0'/c)$.

Quite a different situation takes place for the reflected pulses. In the general case the directions of the wavevector \mathbf{K}_h and the normal \mathbf{N} to the pulse do not coincide (see Appendix C and Fig. 8). This is stipulated by the fact that at a fixed incidence angle θ_0 various spectral components of a field $A_h(\Omega)$ are reflected under different angles $\theta_h(\Omega)$ to the crystal normal. As long as the reciprocal lattice vector \mathbf{h} in \mathbf{k}_h (7) has a non-zero projection $h_x \neq 0$ along the x axis, part of the longitudinal impulse of the wavevector \mathbf{k}_h is transferred to the crystal and the angle of reflection $\theta_h(\Omega)$ is different for various spectral components Ω : $\theta_h(\Omega) = \theta_h + \Delta\theta_h(\Omega)$, where

$$\Delta\theta_h(\Omega) = -2(\Omega/\omega_0) \sin \theta_B \cos \psi / \gamma_h.$$

Superposition of these plane waves gives rise to non-trivial propagation of the reflected pulse in a vacuum. Earlier the speed V_h (22) was not quite correctly named as the 'group velocity' (Malgrange & Graeff, 2003). For a more detailed discussion of this, see Appendix C.

The only exception is the symmetric Bragg case ($b = -1$), for which $\psi = \pi/2$, $\sin \theta_0 = \sin \theta_h$, $\Delta\theta_h = 0$, $V_h = c$ and $D_h = 0$, *i.e.* smearing of pulses in a vacuum does not take place. If $|b| \neq 1$ in the Bragg case, and in any Laue case, $V_h < c$ and the form of the pulse $A_h(t - z'_h/V_h)$ varies during the propagation in a vacuum (Figs. 3–7). For the Laue case, expressions (21) and (22) were given earlier by Malgrange & Graeff (2003) without, however, taking into account the pulse smearing effects, caused by the phase D_h (19), which is quadratic in Ω .

The distance R_D from a crystal along the wavevector \mathbf{K}_h , at which a substantial smearing of the reflected pulse begins, is determined from the condition $|D_h| \simeq 1$, from which $R_D \simeq (\Delta\Omega_E^2 |F_h \gamma_h|)^{-1}$, where in the approximation of the Gaussian forms for $R(\Omega)$ and $A_{\text{in}}(\Omega)$ the effective spectral width $\Delta\Omega_E = \Delta\Omega_0 \Delta\Omega_B / (\Delta\Omega_0^2 + \Delta\Omega_B^2)^{1/2}$. The expression given above for the distance R_D coincides with equation (52) in Appendix C. The effect of smearing and broadening is increased with the reduction of pulse duration, when the incident spectrum width exceeds the spectral width of the Bragg reflection $\Delta\Omega_0 \gg \Delta\Omega_B$ and therefore $\Delta\Omega_E \simeq \Delta\Omega_B$. If, for example, $\tau_0 = 0.1$ fs, then in the Bragg-case Si(220) reflection with $b = -2$ and wavelength $\lambda = 0.154$ nm the distance $R_D \simeq 64$ cm, and in the symmetric Laue case $R_D \simeq 8$ cm (see also Fig. 9).

We shall consider first the reflection of a long incident pulse of duration $\tau_0 \geq \tau_B$ and with small transversal size $r_0 \simeq \Lambda$. Fig. 2 shows the space distributions of the modulus of amplitudes of the incident pulse $|A_{\text{in}}(x_s, z_s)|$ with duration $\tau_0 = 10$ fs (a) and the reflected pulse $|A_h(x_p, z_p)|$ in the symmetric Bragg case (b). In this case the longitudinal size of the pulse $l_0 = \tau_0 c = 3 \mu\text{m}$, as well as its transversal size $r_0 = 10 \mu\text{m}$, are comparable with the X-ray extinction length Λ . Hereinafter the system of coordinates (x_p, z_p) moves together with the reflected pulse [see Fig. 8 and expressions (53), (55)]. After reflection the pulse is strongly stretched in the transverse direction z_p and its maximum intensity decreases by more than four times (Fig. 2a). The degree of distortion of the form of the pulse

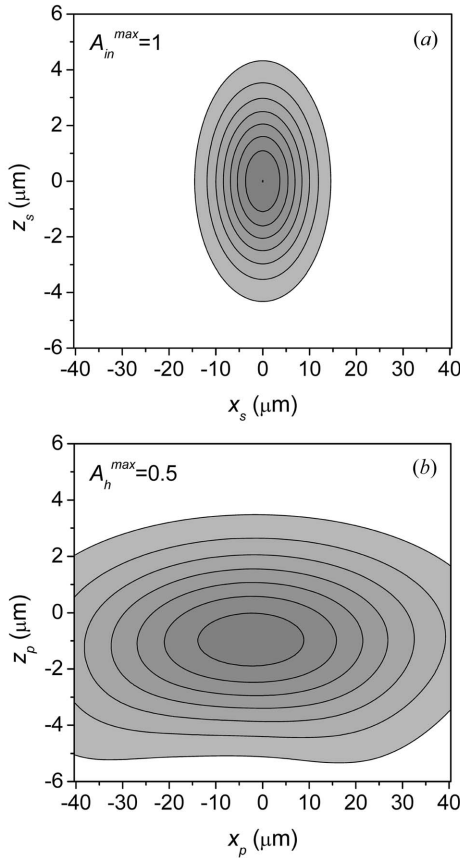


Figure 2
Two-dimensional distribution of the amplitude of a Gaussian incident pulse $|A_{in}(x_s, z_s)|$ (a) and the reflected pulse $|A_h(x_p, z_p)|$ (b) in the symmetric Bragg Si(220) reflection ($b = -1$). Transversal pulse size $r_0 = 10 \mu\text{m}$, pulse duration $\tau_0 = 10 \text{ fs}$ ($l_0 = c\tau_0 = 3 \mu\text{m}$), central wavelength $\lambda = 0.154 \text{ nm}$, thickness of crystal $d = 50 \mu\text{m}$, phase parameter $\alpha_0 = 2$. Angle between the wavevector \mathbf{K}_h and the normal \mathbf{N} to the reflected pulse $\varphi_h = 0$. Distance from the crystal to the reflected pulse $R = 3 \text{ m}$.

increases with increase in distance R from the crystal to the reflected pulse. Meanwhile the size and duration of the reflected pulse in the longitudinal direction remains almost unchanged. This is explained by that fact that the pulse duration τ_0 exceeds the characteristic time $\tau_B = 2/\Delta\Omega_B \simeq 5.8 \text{ fs}$, where for a thick crystal $\tau_B = 2(\Lambda/c)\sin^2\theta_B/|\gamma_h|$. The duration τ_B is defined by a time delay of the waves reflected from a surface of the crystal and from an effective layer of the crystal of depth $z \simeq \Lambda$ [see also expression (6) of Graeff (2004)].

All calculations whose results are shown in Figs. 2–7 are made on the basis of the general formula (9). For clarity, we shall further consider (see Figs. 3–7) the size of the source $r_s = 75 \mu\text{m}$, the parameter of the square-law phase of radiation of a source $\alpha_s = 2$, and the distance from the source to the crystal $z_s = 800 \text{ m}$. Then for an incident pulse we find that $r_0 = 1240 \mu\text{m}$, $\alpha_0 = 36.9$ and angular divergence $\Delta\theta_s = 1.46 \mu\text{rad}$.

It is clear that, starting from some duration of the incident pulse $\tau_0 < \tau_B$, only a part $\Delta\Omega_B < \Delta\Omega_0$ of the incident frequency spectrum $\Delta\Omega_0$ will satisfy the diffraction conditions. This results in a sharp reduction of intensity in the case of short incident pulses in comparison with longer pulses.

As an illustration, Fig. 3 shows the intensity of reflection $I_h(0, z_p)$ of the long and short pulses in the cases of symmetric and asymmetric Bragg reflections. In both cases the intensity of a short pulse after reflection considerably decreases, whereas the long pulse is more weakly deformed. The small peak in the region $z_p = -c(\Delta t_{12} + \tau_B) \simeq -10 \mu\text{m}$ in Fig. 3(a), where $\tau_B = 2(d/c)\sin^2\theta_B/|\gamma_h|$, and Δt_{12} is the time interval between pulses, is connected by reflection of the short pulse from the bottom surface of the crystal (see also Malgrange & Graeff, 2003). In the symmetric Bragg case the intensity of the reflected pulse practically does not change for an increase in the distance R from the crystal to the pulse. At the same time, in the asymmetric Bragg case the maximal intensity of the reflected pulse decreases with an increase in the distance R : its width increases and the contribution of the short pulse to the total intensity becomes extremely small at $R \simeq 0.5 \text{ m}$ (see Fig. 3b).

Moreover, unfortunately for practical applications, for very short femtosecond pulses the duration and shape of a reflected pulse become almost independent of the incident pulse characteristics (Figs. 4–7) (see also Graeff, 2002, 2004; Malgrange & Graeff, 2003). Formally this can be seen from equation (17), as the smooth function $A_{in}(\Omega)$ can be taken outside of the integration. Therefore the form of a pulse on the crystal surface is determined by inverse Fourier transformation of the

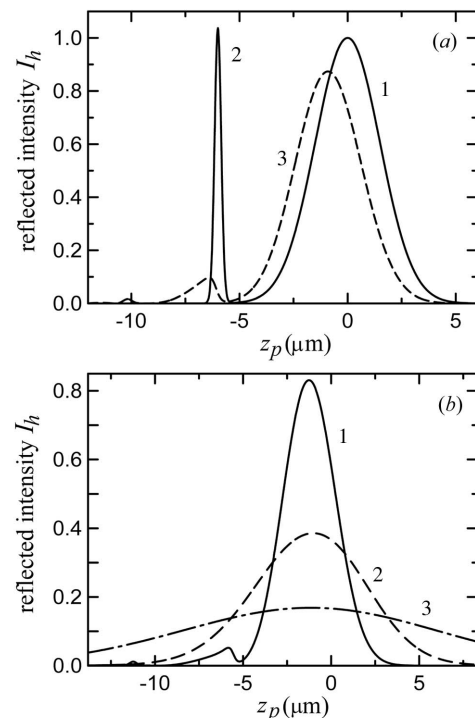


Figure 3
Longitudinal sections of the intensity of reflected pulses $I_h(z_p)$ along the normal \mathbf{N} at $x_p = 0$ in cases of symmetric (a) and asymmetric (b) Bragg reflections. Long ($\tau_{01} = 10 \text{ fs}$) and short ($\tau_{02} = 1 \text{ fs}$) Gaussian pulses with amplitudes $A_1 = A_2 = 1$ [curves 1 and 2 in (a)] are incident on a crystal with time interval $\Delta t_{12} = 20 \text{ fs}$. Thickness of the crystal $d = 5 \mu\text{m}$. (a) Dashed curve 3 is the total reflected pulse, angle $\varphi_h = 0$. (b) Distance from the crystal $R = 0$ (curve 1), $R = 2 \text{ m}$ (curve 2) and $R = 5 \text{ m}$ (curve 3). The asymmetry coefficient of the reflection $b = -2$, critical distance $R_D = 1.6 \text{ m}$, angle of inclination of the reflected pulse $\varphi_h = 23.65^\circ$.

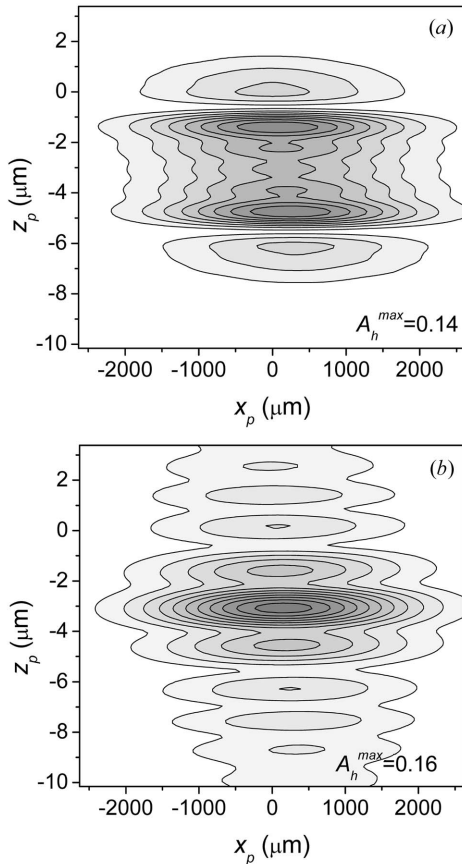


Figure 4 Two-dimensional distribution of amplitude of the reflected pulse $|A_h(x_p, z_p)|$ in the symmetric Laue case ($b = 1$). Distance from the crystal to the pulse $R = 2$ cm (a), and $R = 10$ cm (b). Duration of incident pulse $\tau_0 = 1$ fs, crystal thickness $d = 23.19$ μm , critical distance $R_D = 8.2$ cm, angle of pulse inclination $\varphi_h = -41.2^\circ$. For the incident pulse of longitudinal size $l_0 = 0.3$ μm there appears to be a δ -function on the background of the spatial distribution of the reflected pulse and consequently it is not shown in these figures. Other parameters: size of source $r_s = 75$ μm , phase parameter $\alpha_s = 2$, distance from source to crystal $z_s = 800$ m, transversal size of incident pulse $r_0 = 1240$ μm , phase parameter $\alpha_0 = 36.9$.

reflection coefficient $R(\Omega)$ [as can also be seen in the Green function in Chukhovskii & Förster (1995)].

The second peak in the Bragg case at $z_p \simeq -V_h \tau_B$, where speed V_h is defined in expression (22) and $\tau_B = 2(d/c) \sin^2 \theta_B / |\gamma_h|$, arises owing to reflection from the rear surface of the crystal [see Fig. 6(a) at $z_p \simeq -5.6$ μm , and Fig. 7 (curve 1) at $z_p \simeq -3$ μm]. It is easy to see that any asymmetric Bragg case reflection and any Laue case reflection are not quite acceptable for diffraction tailoring of pulses, because already at distances R as short as 10–30 cm from the crystal the pulses become considerably diffused (Figs. 4–7). The transmitted pulse $I_0(x, z, t)$ meanwhile practically coincides in form and intensity with the incident pulse, as the transmission coefficient $T(\Omega) = \exp(ik_0 \chi_0 d / 2\gamma_0)$ stays constant everywhere except the very narrow spectral slot $|\Omega| \leq \Delta\Omega_B$ [see equations (12) and (14)]. It is obvious that the group of super-short statistically unconnected pulses with total duration $\tau_p < \tau_B$ become merged into one wide asymmetric pulse of duration of the order of τ_B after a reflection (see also Shastri *et al.*, 2001a).

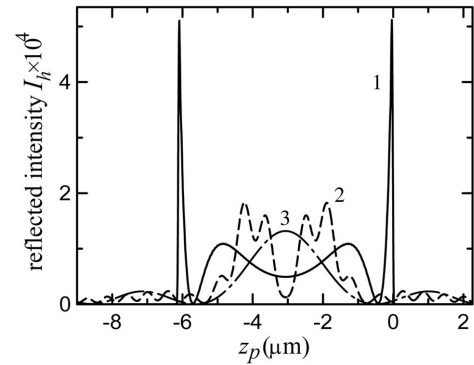


Figure 5 Longitudinal section of intensity of the reflected pulse $I_h(z_p)$ at $x_p = 0$ in the symmetric Laue case ($b = 1$). Distance from crystal to pulse $R = 0$ (curve 1), $R = 5$ cm (curve 2) and $R = 20$ cm (curve 3). Duration of incident pulse $\tau_0 = 0.1$ fs ($l_0 = 0.03$ μm), crystal thickness $d = 23.19$ μm , distance $R_D = 7.9$ cm, angle $\varphi_h = -41.2^\circ$. Other parameters are the same as in Fig. 4.

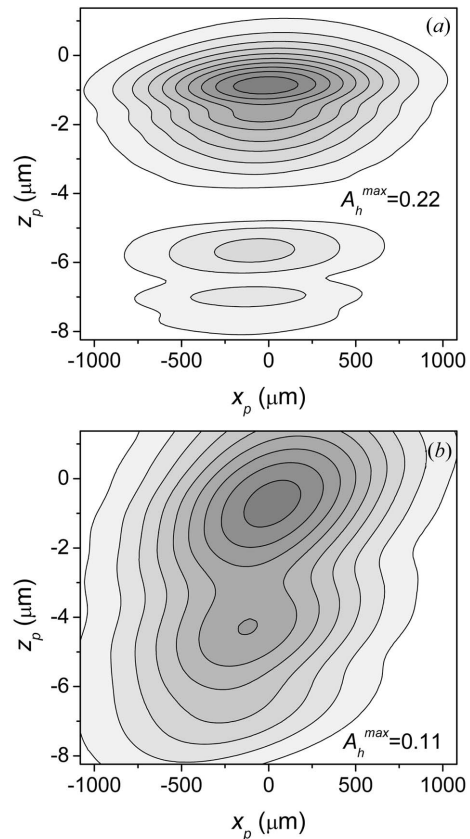
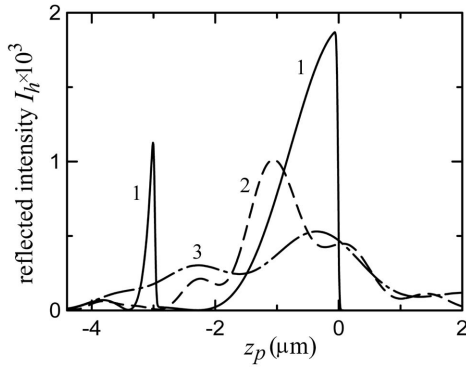


Figure 6 Two-dimensional distribution of amplitude of the reflected pulse $|A_h(x_p, z_p)|$ in the asymmetric Bragg case ($b = -2$). Distance from crystal to pulse $R = 5$ cm (a), and $R = 100$ cm (b). Duration of incident pulse $\tau_0 = 1$ fs, crystal thickness $d = 5$ μm , critical distance $R_D = 64.5$ cm, angle of pulse inclination $\varphi_h = 23.65^\circ$. Other parameters are the same as in Fig. 4.

It is of interest to consider the space and time coherency of XFEL radiation, and the radiation of reflected pulses. The coherence function of an incident pulse is given by

$$\Gamma_{\text{in}}(\rho, \tau) = P^{-1} \left| \left\langle A_{\text{in}}(x, t) A_{\text{in}}^*(x + \rho, t + \tau) \right\rangle \right|, \quad (23)$$


Figure 7

Longitudinal section of intensity of the reflected pulse $I_r(z_p)$ at $x_p = 0$ in the asymmetric Bragg case ($b = -0.5$). Distance from crystal to pulse $R = 0$ (curve 1), $R = 50$ cm (curve 2) and $R = 100$ cm (curve 3). Duration of incident pulse $\tau_0 = 0.1$ fs, crystal thickness $d = 5$ μm , distance $R_D = 63.6$ cm, angle $\varphi_h = -12.35^\circ$. Other parameters are the same as in Fig. 4.

where $P = [I_{\text{in}}(x, t)I_{\text{in}}(x + \rho, t + \tau)]^{1/2}$, $I_{\text{in}}(x, t) = \langle |A_{\text{in}}(x, t)|^2 \rangle$ (angular brackets mean the average over a sufficiently large time interval); $\Gamma_{\text{in}}(0, \tau)$ and $\Gamma_{\text{in}}(\rho, 0)$ are the functions of time and space coherence, respectively, with $\Gamma_{\text{in}}(0, 0) = 1$. According to the calculations of Saldin *et al.* (2004), XFEL pulses are completely coherent over the whole cross section, and the coherence time, which is obtained after substitution of calculated pulses with amplitude and phase modulation in (23), has the value $\tau_c = 0.14$ fs. More convenient for the analysis is the spectral representation,

$$\Gamma_{\text{in}}(\rho, \tau) = I_{\text{in}}^{-1} \left| \iint |A_{\text{in}}(q, \Omega)|^2 \exp[i(q\rho - \Omega\tau)] dq d\Omega \right|, \quad (24)$$

where

$$I_{\text{in}} = \iint |A_{\text{in}}(q, \Omega)|^2 dq d\Omega.$$

It can be shown that the coherence functions of reflected and transmitted pulses are determined by the expression

$$\Gamma_g(\rho, \tau) = I_g^{-1} \left| \iint |B_g(q, \Omega)A_{\text{in}}(q, \Omega)|^2 \times \exp[i(q\rho - \Omega\tau)] dq d\Omega \right|. \quad (25)$$

If in the region of significant variation of the spectrum $A_{\text{in}}(q, \Omega)$ the coefficients $B_g \simeq$ a constant, then the degree of coherence of the reflected pulse $\Gamma_g \simeq \Gamma_{\text{in}}$, *i.e.* the coherence remains preserved. For a short pulse, for which the spectral width $\Delta\Omega_0 \gg \Delta\Omega_B$, the time coherence, as follows from (25), is increased, *i.e.* a partial monochromatization takes place; however, at the same time the pulse intensity decreases.

One of the most serious problems in diffraction of the powerful XFEL pulses will be the very high thermal load on diffracting crystals. So far there is no exact solution for X-ray diffraction taking into account thermal heating, but it is possible to make some estimations. From analysis of the Green function of the thermal conductivity equation with distributed thermal sources in a crystal subsurface layer, it follows that the time of temperature propagation over a distance Δx is $\Delta t \simeq (\Delta x)^2/4a^2$, where $a^2 = \lambda_T/c_T\rho$, λ_T and c_T are coefficients of thermal conductivity and thermal capacity, respectively, and ρ is the crystal density. For silicon at

temperature $T = 300$ K, $\lambda_T \simeq 150$ W m⁻¹ K⁻¹, $c_T \simeq 700$ J kg⁻¹ K⁻¹, $\rho = 2.3$ g cm⁻³ (Grigor'ev & Meilikhova, 1991). For $\Delta x \simeq \Lambda$, one obtains $\Delta t \simeq 13$ ns, and this is much longer than the duration of an X-ray pulse $\tau_0 = 0.1$ –200 fs (for diamond $\Delta t \simeq 20$ ns). Thus it is quite possible that the X-ray laser pulses are simply too short to influence their own diffraction scattering through heating. An increase in temperature of a crystal by $\Delta T = \Delta\theta_B \cot\alpha_T \simeq 10$ K, where α_T is the coefficient of linear expansion (for silicon $\alpha_T = 2.54 \times 10^{-6}$ K⁻¹), results in displacement of the Bragg peak by an angle $\Delta\theta_B$, which is not essential for short pulses with $\Delta\Omega_0 \gg \Delta\Omega_B$.

4. Conclusions

In conclusion, this paper presents a most general approach to the consideration of the diffraction of arbitrary X-ray pulses in crystals and their subsequent dispersion in space. The main attention is devoted to analysis of how space and time change the form and duration of short pulses depending on the distance from the crystal. It is shown that the unique opportunity to avoid distortion of the form and duration of a reflected femtosecond pulse is achieved by use of symmetric reflections in the Bragg diffraction geometry.

APPENDIX A

Calculation of projection k_{gz}

Let us present the values of the wavevectors k_0 and k_{gx} in the expression for k_{gz} in (7) in the following form: $k_0 = K_0(1 + \xi_1)$, where $\xi_1 = \Omega/\omega_0$, and $k_{gx} = K_{gx}(1 + \xi_2)$, where $\xi_2 = q/K_{gx}$. As a result for the square-root expression in (7) we find that

$$k_0^2 - k_{gx}^2 = K_{gz}^2 [1 + 2(a\xi_1 - b\xi_2) + (a\xi_1^2 - b\xi_2^2)], \quad (26)$$

where $K_{gz}^2 = K_0^2 - K_{gx}^2$,

$$a = (K_0/K_{gz})^2 = 1/\gamma_g^2, \quad b = (K_{gx}/K_{gz})^2 = \tan^2 \theta_g. \quad (27)$$

Here $\gamma_g = \cos(\mathbf{K}_g \cdot \mathbf{n}) = \cos\theta_g$, $\mathbf{K}_h = (K_{hx}, \sigma_h |K_{hz}|)$. In the Laue case, $\gamma_h > 0$, and in the Bragg case, $\gamma_h < 0$.

We shall consider now that at $\xi \ll 1$ the following expansion takes place,

$$(1 + \xi)^{1/2} \simeq 1 + (1/2)\xi - (1/8)\xi^2. \quad (28)$$

Then with use of expression (28), from equation (26) we find that

$$\sigma_g(k_0^2 - k_{gx}^2)^{1/2} = K_{gz}(1 + a\xi_1 - b\xi_2) - (1/2)K_{gz} [a(a-1)\xi_1^2 - 2ab\xi_1\xi_2 + b(b+1)\xi_2^2], \quad (29)$$

where $K_{gz} = K_0\gamma_g$. In view of an obvious form of a and b (27) it is easy to see that in (29) factors $a(a-1) = ab = b(b+1) = \tan^2\theta_g/\gamma_g^2$. As a result, from (29) we find finally that

$$k_{gz} = K_{gz} - q \tan \theta_g + (\Omega/c\gamma_g) - [q - (\Omega/c) \sin \theta_g]^2 / (2K_0\gamma_g^3). \quad (30)$$

If now in addition to k_{gz} (30) we consider the x -components of wavevectors \mathbf{k}_g and the item ωt , the phase in the exponential in the integral (6) will have the following form,

$$\mathbf{k}_g \mathbf{r} - \omega t = (\mathbf{K}_g \mathbf{r} - \omega_0 t) + S_g(q, \Omega) + D_g(q, \Omega), \quad (31)$$

where the linear (S_g) and square-law (D_g) phases are set by expressions (10) and (11), respectively.

APPENDIX B

X-ray pulse propagation in free space

The aim of Appendix B is to prove the validity of the form of the Gaussian incident pulse given in (15). In the plane of a source $z_s = 0$ (the exit window of the free-electron laser) is set a field

$$E_s(x_s, t) = A_s(x_s, t) \exp(-i\omega_0 t), \quad (32)$$

where $A_s(x_s, t)$ is the complex slowly varying amplitude of the field, x_s is the transversal coordinate in the plane of the source and ω_0 is the average frequency of radiation. It is required to find the field $E(x_s, z_s, t)$ in any point in space (x_s, z_s) at the moment in time t .

We shall present the field $E_s(x_s, t)$ (32) in the form of an expansion of the Fourier integral over the plane waves,

$$E_s(x_s, t) = \iint E_s(q, \omega) \exp(iqx_s - i\omega t) dq d\omega, \quad (33)$$

where

$$E_s(q, \omega) = (2\pi)^{-2} \iint E_s(x_s, t) \exp(-iqx_s + i\omega t) dx_s dt. \quad (34)$$

Propagation of the pulse field $E(x_s, z_s, t)$ in the region $z_s \geq 0$ is described by the wave equation

$$\Delta E - (1/c^2) \partial^2 E / \partial t^2 = 0, \quad (35)$$

where $\Delta = \partial^2 / \partial x_s^2 + \partial^2 / \partial z_s^2$ is the Laplace operator. In view of the boundary condition for the field $E(x_s, 0, t) = E_s(x_s, t)$ in the plane $z_s = 0$ from (33) and (35) it is easy to see that

$$E(x_s, z_s, t) = \iint E_s(q, \omega) \exp(iqx_s + ik_z z_s - i\omega t) dq d\omega, \quad (36)$$

where $k_z = (k^2 - q^2)^{1/2}$, $k = \omega/c$.

From (32) and (34) it follows that $E_s(q, \omega) = A_s(q, \Omega)$, where $\Omega = \omega - \omega_0$. If the characteristic size of the source $r_s \gg \lambda$, and the pulse duration $\tau_0 \gg T$, where λ is the wavelength of radiation and T is the period, then $q \ll k$ and $\Omega \ll \omega_0$. In this case, with use of the expansion (28) for values of k_z in (36), we have

$$k_z \simeq K_0 + \Omega/c - q^2/2K_0, \quad (37)$$

where $K_0 = \omega_0/c = 2\pi/\lambda$ is an average wavevector of the pulse. Substituting (37) into (36) we find the following expression for the pulse field in a plane z_s ,

$$E(x_s, z_s, t) = A(x_s, z_s, t) \exp(iK_0 z_s - i\omega_0 t), \quad (38)$$

where $A(x_s, z_s, t)$ is the slowly varying amplitude of the pulse,

$$A(x_s, z_s, t) = \iint A_s(q, \Omega) \exp[iqx_s - iq^2 z_s / 2K_0 - i\Omega(t - z_s/c)] dq d\Omega. \quad (39)$$

We shall consider now propagation in space of a Gaussian pulse for which it is possible to find simple analytical expressions. We shall present the amplitude (32) of the field on the source surface $z_s = 0$ in the following form,

$$A_s(x_s, t) = \exp[-(x_s/r_s)^2 + i\varphi_s(x_s) - (t/\tau_0)^2], \quad (40)$$

where r_s is the size of the source in the plane $z_s = 0$, τ_0 is the pulse duration and $\varphi_s(x_s)$ is the phase of the complex amplitude (40). Furthermore we shall consider that this phase is a square-law function of the coordinate x_s , *i.e.* $\varphi_s(x_s) = \alpha_s(x_s/r_s)^2$, where parameter α_s is equal to the phase at $|x_s| = r_s$.

For calculation of the Fourier amplitudes $A_s(q, \Omega)$ in (39) and for calculations of other integrals the known so-called main optical integral (Gradshteyn & Ryzhik, 1980) is used,

$$\int \exp(-i\beta x + i\gamma x^2) dx = (i\pi/\gamma)^{1/2} \exp(-i\beta^2/4\gamma), \quad (41)$$

where β and γ are arbitrary complex values.

Substituting (40) into (34) and (39) leads to the following expression for the pulse amplitude at any plane z_s ,

$$A(x_s, z_s, t) = A_s \exp[-(x_s/r_0)^2 + i\varphi_0(x_s) - (t - z_s/c)^2/\tau_0^2 + i\Phi_0], \quad (42)$$

where $A_s = 1/M^{1/2}$, $M = [(1 + \alpha_s W)^2 + W^2]^{1/2}$, $W = \lambda z_s / \pi r_s^2$ is the wave parameter,

$$\begin{aligned} r_0 &= r_s M, & \varphi_0(x_s) &= \alpha_0 (x_s/r_0)^2, \\ \alpha_0 &= \alpha_s + (1 + \alpha_s^2)W, & & \\ \Phi_0 &= -(1/2) \arctan[W/(1 + \alpha_s W)]. \end{aligned} \quad (43)$$

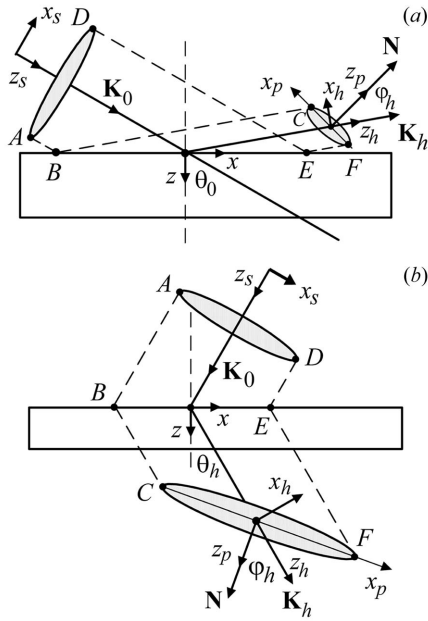
From expression (42) we can see that the initial Gaussian pulse keeps its form and duration in the process of propagation in space; however, the transversal size of the pulse $r_0(z_s)$ increases M times in comparison with r_s with increase in distance z_s and with increase in phase parameter α_s . This phase parameter describes an initial curvature of the wavefront. The phase of the pulse $\varphi_0(x_s)$, also a square-law function, depends on the transversal coordinate. The parameter of this phase $\alpha_0(z_s)$ increases with increase in distance z_s and with increase in parameter α_s , and also increases with reduction of the source size r_s . The phase parameter $\alpha_0 \neq 0$, even at the initial plane wavefront, *i.e.* at $\alpha_s = 0$. The phase $\Phi_0(z_s)$ does not depend on the transversal coordinate x_s and does not play an essential role during propagation and diffraction of the pulse. Later we shall consider for simplicity that in (42) $A_s = 1$, $\Phi_0 = 0$.

The width of the angular spectrum of a pulse (42) $\Delta\theta_s = \Delta q_s / K_0$, *i.e.* the width of the function $|A(q, \Omega, z_s)| \simeq \exp[-(q/\Delta q_s)^2]$, where $\Delta q_s = 2(1 + \alpha_0^2)^{1/2}/r_0 = 2(1 + \alpha_s^2)^{1/2}/r_s$, does not depend on the distance z_s and is determined by the expression

$$\Delta\theta_s = (\lambda/\pi r_s)(1 + \alpha_s^2)^{1/2}. \quad (44)$$

The angular width $\Delta\theta_s$ (44) in the general case exceeds the diffraction divergence $\Delta\theta_d = (\lambda/\pi r_s)$, related only to the size of the source r_s .

Theoretical calculations show (Saldin *et al.*, 2004) that on exit from undulator SASE1 ($\lambda \simeq 0.1$ nm) the full width of the pulse at half-height is equal to 90 μm , and the angular diver-


Figure 8

Geometry in real space of an asymmetric Bragg case (a) and Laue case (b) diffraction. Here \mathbf{K}_0 and \mathbf{K}_h are the average wavevectors of the incident and reflected pulses, respectively; \mathbf{N} is the normal to the long axis of the reflected pulse; (x_s, z_s) is a Cartesian system of coordinates on the source surface, (x, z) is a system of coordinates on the crystal surface, the system of coordinates (x_h, z_h) moves together with the reflected pulse, axis z_h is directed along the wavevector \mathbf{K}_h ; axes of the moving system of coordinates (x_p, z_p) are directed along the main axes of the pulse, φ_h is an angle between the normal \mathbf{N} to the reflected pulse and the direction of pulse propagation \mathbf{K}_h .

gence of the beam is equal to 1.1 μrad . In our notation this means that $r_s \simeq 76.4 \mu\text{m}$ and $\Delta\theta_s \simeq 0.93 \mu\text{rad}$. From here and (44) it follows that the phase parameter $\alpha_s \simeq 2$. Then with use of formulae (43) it is easy to show that at the distance $z_s = 800 \text{ m}$ the transversal pulse size $r_0 \simeq 820 \mu\text{m}$, and the phase parameter $\alpha_0 \simeq 24$.

The relation between coordinates (x_s, z_s) on the source of an X-ray pulse and coordinates (x, z) on the crystal surface is determined by means of the following expressions: $x_s = x \cos \theta_0 - z \sin \theta_0$, $z_s = x \sin \theta_0 + z \cos \theta_0 + z_1$, where θ_0 is the incident angle of the pulse on the crystal with respect to the normal \mathbf{n} to the crystal surface, and z_1 is the distance from the source to the crystal (see Fig. 8). Then the amplitude of the field (42) on the crystal surface $z = 0$ will be

$$A_{\text{in}}(x, t) = \exp\left[-(x\gamma_0/r_0)^2(1 - i\alpha_0) - (t - x \sin \theta_0/c)^2/\tau_0^2\right], \quad (45)$$

where $\gamma_0 = \cos \theta_0$, and the time t is counted from the moment $t_1 = z_1/c$ of incidence of the pulse maximum at $x = 0$, $z = 0$ on the crystal.

APPENDIX C

Reflection of a Gaussian pulse

We shall consider diffraction reflection of the incident pulse $A_{\text{in}}(x, t)$ (45) from the crystal. From the expression (45) in view

of (41) we find the following expression for Fourier amplitudes of the incident pulse in (9),

$$A_{\text{in}}(q, \Omega) = A_0 \exp\left[-(q - \Omega \sin \theta_0/c)^2(1 + i\alpha_0)/\Delta q_0^2 - (\Omega/\Delta\Omega_0)^2\right], \quad (46)$$

where $\Delta\Omega_0 = 2/\tau_0$ is the spectral width of the incident pulse, $\Delta q_0 = 2\gamma_0(1 + \alpha_0^2)^{1/2}/r_0$ is the width of the angular spectrum in q -space, and amplitude $A_0 = (1 + i\alpha_0)^{1/2}/(\pi\Delta q_0\Delta\Omega_0)$. It is easy to show that $\Delta q_0 = \gamma_0\Delta q_s$, where $\Delta q_s = 2(1 + \alpha_s^2)^{1/2}/r_s$ is the width of the angular spectrum of the pulse in the plane $z_s = 0$ of the source.

For simplicity of the analysis of the form and the orientation of the reflected pulse we shall present the amplitude reflection coefficient $R(q, \Omega)$ in the integral (9) in the form of a Gaussian function [see argument $\alpha(q, \Omega)$ (13) in (12) and (14)],

$$R(q, \Omega) = \exp\left\{-[q - (\Omega/c) \sin \psi / \cos \theta_B]^2 / \Delta q_B^2\right\}, \quad (47)$$

where $\Delta q_B = K_0\gamma_0\Delta\theta_B$ is the width of the diffraction reflection curve.

We shall now substitute $A_{\text{in}}(q, \Omega)$ (46) and $R(q, \Omega)$ (47) into the general integral equation (9) for the amplitude of the reflected pulse, where $g = h$. As a result, using (41) we find that

$$A_h(x, z, t) = A_R \exp\left[-\Phi_1^2(1 - i\alpha_0) - \Phi_2^2(1 - i\beta_0)\right], \quad (48)$$

where

$$\Phi_1 = (x - z \tan \theta_h)\gamma_0/r_0, \quad (49)$$

$$\Phi_2 = [t - z/c\gamma_h - (x - z \tan \theta_h) \sin \theta_0/c]/\tau_R. \quad (50)$$

Here, τ_R is the duration of the reflected pulse, which is determined by the following formula,

$$\tau_R = \tau_E(1 + \beta_0^2)^{1/2}, \quad (51)$$

where

$$\tau_E = (\tau_0^2 + \tau_B^2)^{1/2}, \quad \tau_B = 2/\Delta\Omega_B, \quad (51a)$$

$$\Delta\Omega_B = \omega_0\Delta\theta_B \cotan \theta_B,$$

$$\beta_0 = (\tau_Z/\tau_E)^2, \quad \tau_Z = 2(F_h z)^{1/2}, \quad (51b)$$

$$F_h = (\sin \theta_0 - \sin \theta_h)^2 / (2K_0 c^2 \gamma_h^3),$$

$$A_R = (\tau_0/\tau_R)(1 - i\beta_0)^{1/2}. \quad (51c)$$

In order to obtain expression (48) it is considered that the ratio $\Delta q_0/\Delta q_B = \Delta\theta_s/\Delta\theta_B \ll 1$, where $\Delta\theta_s = (\lambda/\pi r_s)(1 + \alpha_s^2)^{1/2}$ is the width of the angular spectrum of the source radiation, and distance $|z| \ll z_F$, where $z_F = \pi r_0^2/[\lambda b^2(1 + \alpha_0^2)]$.

From equations (51) it follows that the pulse duration τ_R after reflection from the crystal increases in comparison with τ_0 for two reasons. The first reason is related to the finite quantity of the spectral width $\Delta\Omega_B$ of the Bragg reflections. For sufficiently short pulses the spectral width $\Delta\Omega_0 > \Delta\Omega_B$, and therefore $\tau_B > \tau_0$. The second reason is connected to diffusion broadening of the part of the pulse duration τ_Z on increasing the distance from the crystal to the reflected pulse along the wavevector \mathbf{K}_h . From the characteristic distance R_D ,

at which the intensity of the pulse $|A_R|^2$ will decrease twice, it is possible to estimate from the equation $\beta_0 = 1$,

$$R_D = (\tau_0^2 + \tau_B^2)/4|F_h\gamma_h|. \quad (52)$$

From equation (52) it follows that diffusion broadening of the pulse is absent only in the case of symmetric Bragg reflection ($b = -1$), at which $\sin\theta_0 = \sin\theta_h$, $F_h = 0$ and $R_D \rightarrow \infty$. The critical distance R_D (52) increases with increase in τ_0 , if $\tau_0 > \tau_B$ (see Fig. 9). The dependence of the value τ_B from the asymmetry coefficient of reflection b is shown in the insert of Fig. 9. For short pulses with $\tau_0 \ll \tau_B$ the distance R_D does not depend on the duration of the incident pulse τ_0 . Unfortunately in practice the distance R_D does not exceed several tens of centimetres in the Laue case at $\tau_0 \leq 1\text{--}10$ fs (see Fig. 9).

From the form of arguments Φ_1 and Φ_2 in (48) we can see that the reflected pulse $A_h(x, z, t)$ propagates with the speed of light c in a vacuum along the direction of the wavevector \mathbf{K}_h . The orientation of the pulse in space is determined mainly by the angles θ_0 and θ_h , *i.e.* by the asymmetry coefficient of the reflection b .

For analysis of this, we shall pass to the system of coordinates (x_h, z_h) , which moves together with the pulse, and the axis z_h is directed along the wavevector \mathbf{K}_h , *i.e.* this coordinate system is turned in relation to the laboratory system of coordinates (x, z) by angle θ_h (see Fig. 8),

$$\begin{aligned} x &= ct \sin\theta_h + x_h \cos\theta_h + z_h \sin\theta_h, \\ z &= ct \cos\theta_h + z_h \cos\theta_h - x_h \sin\theta_h. \end{aligned} \quad (53)$$

Then the functions $\Phi_{1,2}$ in (48) will have the following form,

$$\Phi_1 = bx_h/r_0, \quad \Phi_2 = (a_{0h}x_h + z_h)/(c\tau_R), \quad (54)$$

where $a_{0h} = (\sin\theta_0 - \sin\theta_h)/\gamma_h$.

From equations (54) it can be seen that only in the symmetric Bragg geometry when $\sin\theta_0 = \sin\theta_h$ and $a_{0h} = 0$ do the axes of the reflected pulse coincide with axes x_h and z_h . In all other cases the pulse propagates so that its axes are inclined by some angle φ_h relative to the direction of propagation \mathbf{K}_h (see Fig. 8).

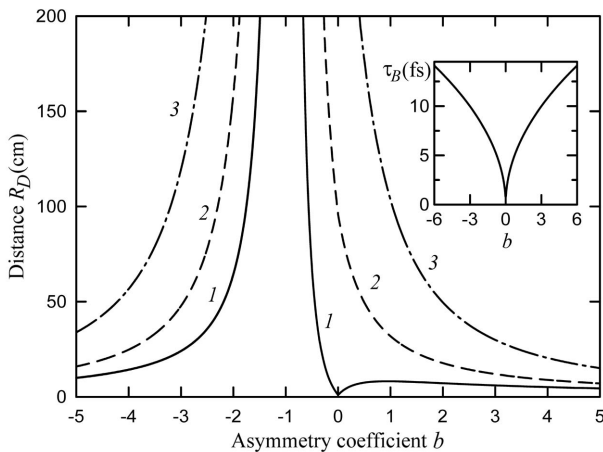


Figure 9 Dependence of the critical distance R_D on the asymmetry coefficient of reflection b at various durations of the incident pulse τ_0 : curve 1, 1 fs; curve 2, 10 fs; curve 3, 20 fs; σ -polarization.

We shall consider the most interesting case of a wide and short pulse, whose transversal size r_0 is much larger than its longitudinal size $l_0 = c\tau_0$, incident on a crystal. In order to find the angle φ_h between the normal \mathbf{N} to the long axis of the reflected pulse and the direction of distribution \mathbf{K}_h we shall pass to a new system of coordinates (x_p, z_p) by means of equations

$$\begin{aligned} x_h &= x_p \cos\varphi_h + z_p \sin\varphi_h, \\ z_h &= x_p \sin\varphi_h - z_p \cos\varphi_h. \end{aligned} \quad (55)$$

The angle φ_h is obtained from the condition that the coefficient of product $x_p z_p$ in the expression $\Phi_1^2 + \Phi_2^2$ in (48) equals zero. As a result we find that

$$\tan\varphi_h = a_{0h}(1 + \delta), \quad (56)$$

where $\delta = (bc\tau_R/r_0)^2/(1 + a_{0h}^2) \ll 1$. The dependence of the angle of inclination φ_h of the reflected pulse from the asymmetry coefficient of the reflection b is shown in Fig. 10.

So, the modulus of the amplitude of the reflected pulse in a moving system of coordinates (x_p, z_p) is

$$|A_h(x_p, z_p)| = (\tau_0/\tau_R) \exp[-(x_p/r_T)^2 - (z_p/r_L)^2], \quad (57)$$

where $r_T = r_0/(|b|\cos\varphi_h)$ is the transversal size of the pulse and $r_L = V_L\tau_R$ is the longitudinal size of the pulse. Here $V_L = c\cos\varphi_h$ is a projection of the pulse speed \mathbf{c} on the axis z_p . Expression (57) represents, figuratively speaking, an instant photo-picture of the reflected pulse in the moment of time $t = z/c\gamma_h$. From equation (56) it is easy to see that

$$\cos\varphi_h \simeq |\gamma_h|/(1 - 2\sin\theta_0\sin\theta_h + \sin^2\theta_0)^{1/2}. \quad (58)$$

This expression can be found also from the condition of equality of the optical paths $L_{ABC} = L_{DEF}$ (see Fig. 8).

Earlier (Malgrange & Graeff, 2003) the speed V_L was not quite correctly referred to as the group velocity. Such a discrepancy has arisen because in this work the incident and reflected pulses were considered infinite in the transversal direction along the axis x_p (*i.e.* $r_0 \rightarrow \infty$). For this reason

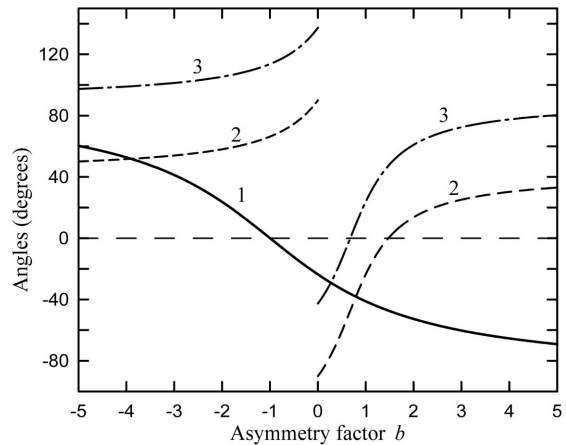


Figure 10 Dependence of the inclination angle of the reflected pulse φ_h (1), of the incident angle θ_0 (2), and of the reflected angle θ_h (3) on the asymmetry coefficient of the reflection b .

propagation of the reflected pulse with projection speed $V_T = c \sin \varphi_h$ along this transversal direction could not be considered in principle.

The most important, and rather unfavourable for practical applications, feature of short X-ray pulse diffraction is the inclination of the reflected pulse relative to the propagation direction (see Figs. 8 and 10). The real pulse duration τ_{tot} , i.e. the time of its passage through a plane, perpendicular to wavevector \mathbf{K}_h , will be determined both by angle of inclination φ_h and by projection $r_0/|b|$ onto this plane of the transversal size of the pulse: $\tau_{\text{tot}} = (r_0/c)|\sin \varphi_h/b|$. If, for example, $r_0 = 800 \mu\text{m}$, $b = 1$, then the angle of inclination $\varphi_h = -41.2^\circ$ and the total duration of the reflected pulse $\tau_{\text{tot}} = 2 \times 10^3$ fs, which exceeds the duration of the incident femtosecond pulse by some orders.

The author is very grateful to D. Novikov for helpful discussions. The work was supported by the Russian Foundation Base Research (Grants No. 06-02-17249, No. 07-02-00324) and the International Science and Technology Center (Project No. 3124).

References

- Afanas'ev, A. M. & Kohn, V. G. (1971). *Acta Cryst.* **A27**, 421–430.
- Altarelli, M. *et al.* (2006). Editors. Report DESY 2006–097. DESY, Hamburg, Germany. (http://xfel.desy.de/tdr/index_eng.html.)
- Arthur, J. *et al.* (2002). LCLS Conceptual Design Report. LCLS, USA. (<http://www-ssrl.slac.stanford.edu/lcls/cdr/>.)
- Bauspiess, W., Bonse, U. & Graeff, W. (1976). *J. Appl. Cryst.* **9**, 68–80.
- Chukhovskii, F. N. & Förster, E. (1995). *Acta Cryst.* **A51**, 668–672.
- Gradshteyn, I. S. & Ryzhik, I. M. (1980). *Table of Integrals, Series and Products*. New York: Academic Press.
- Graeff, W. (2002). *J. Synchrotron Rad.* **9**, 82–85.
- Graeff, W. (2004). *J. Synchrotron Rad.* **11**, 261–265.
- Grigor'ev, I. S. & Meilikhova, E. Z. (1991). Editors. *Physical Values. Handbook*. Moscow: Energoatomizdat. (In Russian.)
- Malgrange, C. & Graeff, W. (2003). *J. Synchrotron Rad.* **10**, 248–254.
- Saldin, E. L., Schneidmiller, E. A. & Yurkov, M. V. (2004). Report TESLA-FEL 2004–02. DESY, Hamburg, Germany.
- Shastri, S. D., Zambianchi, P. & Mills, D. M. (2001a). *J. Synchrotron Rad.* **8**, 1131–1135.
- Shastri, S. D., Zambianchi, P. & Mills, D. M. (2001b). *Proc. SPIE*, **4143**, 69–77.
- Slobodetskii, I. Sh. & Chukhovskii, F. N. (1970). *Kristallografiya*, **15**, 1101–1107. (In Russian.)
- Tanaka, T. & Shintake, T. (2005). *SCSS X-FEL Conceptual Design Report*, edited by Takashi Tanaka and Tsumoru Shintake. SCSS XFEL, R&D Group, RIKEN Harima Institute/SPring-8, Japan. (<http://www-xfel.spring8.or.jp/SCSSCDR.pdf>.)
- Wark, J. S. & He, H. (1994). *Laser Part. Beams*, **12**, 507–513.
- Wark, J. S. & Lee, R. W. (1999). *J. Appl. Cryst.* **32**, 692–703.